Perpendicular anisotropy and spin reorientation in epitaxial $Fe/Cu_3Au(100)$ thin films

F. Baudelet*
Laboratoire de Métallurgie Physique & Science des Matériaux, F-54042 Nancy Cédex, France

M.-T. Lin, W. Kuch, K. Meinel, B. Choi,† C.M. Schneider,‡ and J. Kirschner
Max-Planck-Institut für Mikrostrukturphysik, Weinberg 2, D-06120 Halle, Germany
(Received 14 November 1994; revised manuscript received 26 January 1995)

The *in situ* magneto-optical Kerr effect in both the polar and longitudinal geometry is studied for fcc Fe films on $Cu_3Au(100)$ between 1.7 and 7.5 atomic layers thick. In films with Fe coverages less than 4 monolayers (ML) we observe a perpendicular magnetic anisotropy at temperatures below 300 K. At T=160 K the films exhibit a continuous spin reorientation transition from a perpendicular to an in-plane magnetization in a narrow thickness range between 3.5 and 4 ML. According to the thickness dependence of the Kerr signal the individual layers order ferromagnetically, in contrast to the findings in the Fe/Cu(100) system. Distinct changes in the magnetic properties as a function of coverage may be related to different states of the film structure and morphology.

I. INTRODUCTION

The presence of magnetic long-range order and the size of the magnetic moment in iron depends sensitively on the crystallographic structure and interatomic distances.[1,2] An extensive theoretical work predicts several stable electronic phases for fcc iron as a function of the lattice constant.[1,3–6] Each of these phases is characterized by a different magnetic moment. One distinguishes a high-spin magnetic state ($2.3\mu_B$/atom) connected to a high-volume phase (lattice constant $a_0 \geq 3.6$ Å) from two low-spin states.[7,8] The low-spin state (LS1) partially overlaps in its allowed range of lattice constants ($3.58 \leq a_0 \leq 3.66$ Å) with the high-spin state and is predicted to have a magnetic moment between $0.75\mu_B$/atom and $1.6\mu_B$/atom. A second low-spin state (LS2) is found in theory at even lower lattice constants with a magnetic moment of about $0.5\mu_B$/atom. Other calculations predict a monotonous increase of the magnetic moment with the lattice constant.[9] It should be kept in mind that since these calculations often yield local magnetic moments, they usually cannot predict the type of magnetic ordering, i.e., whether the system orders ferromagnetically or antiferromagnetically. Although there is some indication, both from experiment and theory, that the ground state of fcc iron may be antiferromagnetically ordered, it is not yet clear how this ordering is affected by systematic changes of the lattice constant.

The stable phase of iron at normal pressure and room temperature is bcc with a strong ferromagnetic order. There is even evidence from theory that the ferromagnetism may stabilize the bcc lattice structure.[7] The bulk fcc iron phase appears between 1183 and 1663 K, which is already well above the bulk Curie temperature. Studies on magnetic properties of fcc iron at room temperature are therefore practically impossible on bulk samples. Two different techniques have been developed and employed in order to approach the problem and arrive at a characterization of fcc iron. The first method investigates small Fe precipitates in a Cu matrix. The iron particles predominantly assume the fcc lattice of the host crystal.[10] Their magnetic ordering is determined to be antiferromagnetic. The Néel temperature T_N is found to increase with the particle size up to a maximum of T_N=67 K. The other approach exploits the recent developments in metallic thin-film epitaxy by growing one or several atomic layers under well-defined conditions. In recent years, the interest has concentrated on iron films deposited by molecular-beam epitaxy onto suitable fcc substrates, these being mostly the low-indexed faces of Cu.[11–13] Particularly the Fe/Cu(100) system, which exhibits a perpendicular magnetization, received wide interest regarding both magnetic[11,13–19] and structural aspects.[20–32] A critical compilation of the results of the individual studies draws a complex picture of the correlations between growth, crystalline structure, and magnetic properties. The extreme sensitivity of the system to the various physical parameters during the preparation and even analysis of the films may explain some of the controversies in the early phase of these investigations.

Some of these controversies have been attributed to the fact that the lattice constant of Cu (a_0=3.61 Å) lies in a region where the high-spin (HS) and low-spin state (LS1) may coexist, thus giving an ambiguous solution for the magnetic moment. The specific advantage of thin-film epitaxy is the possibility to choose the crystallographic orientation and the lattice parameter of the substrate. This offers a chance to create metastable phases like fcc iron with various lattice parameters at room temperature. These may result in either an expanded or compressed structure relative to the equilibrium value, provided that a suitable substrate has been chosen.[3] Starting from pure copper, various Cu-based alloys can be used for this purpose. An increase of the lattice constant is

obtained, for example, by alloying Cu with Au. At a concentration of 25 at. % gold, this system forms a stable fcc-like phase, Cu_3Au, with single crystals large enough to serve as templates for epitaxial growth. The lattice constant of Cu_3Au is about $a_0=3.75$ Å.[33] Translating this lattice constant into fcc iron leads to a structure in which, according to the majority of the theoretical predictions, solely the high-spin (HS) state prevails. Therefore, recently some investigations have been devoted to the growth of Fe films on $Cu_3Au(100)$.[34,35] In particular, by comparison of Fe/Cu(100) and Fe/Cu_3Au(100) one should expect further insight into the various physical parameters that determine the magnetic behavior of fcc iron. Nevertheless, it is still an open question as to how closely the electronic and magnetic properties of quasi-two-dimensional metastable phases reflect the bulk properties of the respective material. For example, the Curie temperature in thin films is often found to be dramatically lower than the bulk value[36] and may depend strongly on the film thickness and structure.[37,38] One therefore has to know in detail about the real structure of the grown films and the interaction with the specific substrate in order to understand their genuine magnetic properties.

One of the two major issues in the magnetism of ultrathin films is the onset and presence of long-range magnetic order. Mermin and Wagner predicted the total absence of ferromagnetism or antiferromagnetism in one- or two-dimensional isotropic Heisenberg models.[39] Nevertheless, there is a great body of experimental evidence today that long-range magnetic order exists in two dimensions, though often at reduced critical temperatures.[36–38,40] In their theorem Mermin and Wagner assumed the magnetic interactions to be short-ranged and belonging to a group symmetry. The last requirement is only fulfilled in the absence of anisotropies. Magnetic anisotropies form the other major issue of thin-film magnetism. A lot of contemporary theoretical efforts describe the nature of magnetic order in two-dimensional systems on the basis of extended Heisenberg models,[41–45] Ising models,[46,47] or spin waves.[48–51] Most of the recent approaches now incorporate exchange, magnetic dipolar interactions, electronic hybridization with the substrate, and, most important, surface anisotropy due to spin-orbit interaction, which was neglected in the original work by Mermin and Wagner. The results led to the conclusion that ultrathin films per se must be considered as anisotropic magnetic systems.

The surface contribution to the anisotropy may play a key role in the magnetic properties of thin films. It was suggested by Néel[52] that the broken symmetry at the surface can lead to a higher magnetocrystalline anisotropy. Particularly for a cubic crystal where the first nonzero term in the bulk anisotropy energy[53] is a fourth-order term, a second-order term appears only at the surface, where the symmetry is no longer cubic. Phenomenologically, the influence of the surface anisotropy on the total anisotropy of a magnetic thin film is sometimes assumed to decrease like $1/t$, where t is the layer thickness. This only holds if the surface anisotropy is independent of the film thickness, and may not always be true for very thin films in the monolayer limit. Because it is based on localized magnetic moments, the original model developed by Néel is not well adapted to itinerant magnetism (3*d* transition metals). Other approaches, which include spin-orbit coupling in the framework of band theory,[54,55] are more applicable for this purpose. Nevertheless, with his model Néel was able to predict, 20 years before the first experimental evidence,[56] that surface anisotropy can sometimes cause an orientation of the magnetization perpendicular to the film plane (perpendicular anisotropy). This surface anisotropy competes with the dipolar anisotropy (also called shape anisotropy or demagnetizing field), which tends to keep the magnetization within the film plane (in-plane anisotropy).[57] The dipolar anisotropy depends on the total magnetization of the film and increases therefore with film thickness. In the case of a perpendicular anisotropy at low coverages, there will be a critical thickness at which the shape anisotropy overcompensates the perpendicular contribution, thus causing a spin reorientation. This has been shown experimentally in various systems: Fe/Cu(100) (Refs. 11, 13, and 57) and Fe/Ag(100) (Ref. 58), and has been theoretically discussed.[41,48,59] The picture may be more complicated, however, if thickness-dependent changes of the anisotropy constants are involved, as has been observed in Ni films on Cu(100).[60] Another difficulty encountered in predicting the magnetic anisotropy of thin films is the contribution of the surface roughness, which modifies the surface anisotropy[57] and magnetoelastic anisotropy contributions in the case of large lattice mismatch.[61]

The subject of the present paper is the magnetic properties of thin fcc Fe(100) films epitaxially grown on a $Cu_3Au(100)$ substrate and their relationship with structural particularities. The considerable lattice mismatch of 4.2% favors a fcc structure of iron with a nonzero magnetic moment.[5] As has been mentioned above, this system was already studied by Rochow *et al.*,[34] who measured only in-plane magnetized films. They performed spin-polarized secondary-electron spectroscopy and found a zero-spin polarization component parallel to the film plane for films thinner than 3.6 ML. It is highly unlikely that Fe should not have a magnetic order below this thickness and as pointed out by Pescia *et al.*[62] an experiment measuring a signal proportional to the in-plane remanent magnetization cannot distinguish between a nonmagnetic state and perpendicular remanence. For these reasons and the arguments developed in the Introduction, we therefore expected to find perpendicular anisotropy for fcc Fe monolayers on $Cu_3Au(100)$. Our magneto-optical Kerr effect experiments indeed confirm the presence of a perpendicular anisotropy for a certain thickness and temperature range.

II. EXPERIMENTAL SETUP

The experiments were carried out *in situ* in an UHV chamber (base pressure 2×10^{-8} Pa) equipped with facilities for low-energy electron diffraction (LEED), Auger electron spectroscopy (AES), magneto-optical Kerr effect (MOKE), and thin-film growth. The AES system com-

prised a cylindrical mirror analyzer with an integral electron gun. It was mounted face to face with the LEED system, so that the electron beam of the AES could be displayed on the LEED fluorescent screen. The geometry permits diffraction experiments in a grazing incidence geometry with primary electron kinetic energies up to 10 keV. The angle of incidence varies between 2° and 5°, depending on the primary electron energy and the diffraction conditions chosen. This medium energy electron diffraction (MEED) is employed to monitor the process of epitaxial growth by recording the intensity of selected diffraction beams as a function of deposition time.[37] The water-cooled electron-beam evaporation sources are operated without crucibles in order to avoid contamination. The electron beam is directly focused onto the tip of a high-purity Fe wire. After proper outgassing of the wire, mainly from nitrogen, the pressure during evaporation could be kept below 5×10^{-8} Pa at evaporation rates of several monolayers per minute. The evaporation source is equipped with a flux monitor, which measures the ionized fraction of the outgoing particles. For sample cleaning procedures, the chamber is equipped with a differentially pumped ion gun, which permits us to maintain a vacuum of about 10^{-5} Pa in the chamber during ion bombardment.

The MOKE setup employs a UHV-compatible coil with a soft iron core driven by a computer controlled bipolar power supply. The magnet can be moved along the coil axis in order to accommodate various sample positions. The maximum accessible field at the sample is about 400 Oe. The optical part of the MOKE apparatus consists of two He-Ne lasers operated at a wavelength of λ=633 nm. Each of them is equipped with an electro-optical modulator. The latter device introduces a periodic modulation of the light polarization, which allows a detection of the Kerr signal by a lock-in technique. This ensures a good signal-to-noise ratio mandatory for a sufficient sensitivity at small coverages. The Kerr rotation in the reflected light is measured by a compact combination of polarization filter, interference filter, and integrated photodiode-amplifier chip. The lasers are arranged in such a way that both the polar and longitudinal Kerr effect can be measured by simply rotating the sample around its vertical axis. This way we can use the same light detector for both optical paths. In the longitudinal setup the laser beam passes through a bore in the core of the magnet before it is reflected at the sample surface. The angle of incidence with respect to the surface is $\Theta = 10°$. In the polar geometry the rear of the sample faces the magnet so that the field axis is normal to the surface. The laser beam comes in at an angle of $\Theta = 19°$ relative to the surface normal. Because of this geometry, polar and longitudinal Kerr effects can be measured quasisimultaneously without any rearrangement of the optical elements, thus improving speed and reproducibility of the measurements. This is an important aspect when working on systems with a spin-reorientation behavior.

III. TEMPLATE PREPARATION

The template used for growing the ultrathin iron films was a (001) face of a disk-shaped Cu_3Au single crystal. In order to have a high reflectivity in the MOKE experiments, the crystal surface was polished to an optical flatness of less than 0.1 μm. The orientation of the surface normal agreed with the (001) crystallographic direction to better than 0.5° as checked by Laue procedures. The mosaic spread of the alloy crystal was also found to be less than 0.5°. After insertion into the vacuum chamber, the surface was treated by cycles of Ar^+ ion bombardment (20 min at 1.5 keV) and annealing (900 K, 15 min). This procedure was repeated for a period of approximately 50 h, after which the concentration of the bulk contaminants (mainly sulfur and carbon) had dropped below the detection limit of the AES (~2% of a monolayer). This as-prepared state yields a LEED pattern with predominantly $p(1\times1)$ symmetry, and weak $c(2\times2)$ superstructure spots. The $c(2\times2)$ superstructure is due to the chemical ordering in the Cu_3Au alloy that sets in below 663 K. Above this critical temperature the crystal structure may be described as a simple fcc lattice with 75% (25%) probability of finding a Cu (Au) atom at a given lattice site. Below 663 K the crystal assumes a L_{12} structure, which can be visualized by an fcc unit cell with gold atoms at the cube corners and copper atoms in the center of each face of the cube. In order to improve the degree of chemical order within the Cu_3Au crystal, it was annealed to ~600 K for 30 min. This additional step led to a significant increase of the intensity of the $c(2\times2)$ superstructure spots and yielded extra spectral features in spin-resolved photoemission experiments,[63] indeed indicating an improvement of the near-surface chemical order. According to AES results the well-ordered surface (in the structural and chemical sense) showed a bulklike stoichiometry in the near-surface region, with no noticeable surface segregation of one of the alloy constituents. This is in agreement with previous experiences on this particular alloy surface.[64]

Seen along the [001] direction, a perfect Cu_3Au crystal consists of alternating lattice planes of pure Cu and $Cu_{0.5}Au_{0.5}$. Upon simple truncation of the bulk L_{12} crystal structure, one thus finds two possible configurations for the (001) surface: a 100% Cu surface and a Au-rich surface with 50% gold concentration. A previous ion scattering experiment at higher energies determined the concentration ratio in the topmost layer to be close to Au/Cu=1/1,[64] whereas a recent low-energy ion scattering study found the surface to be Au rich, without giving an experimental value for the Au concentration.[65] It must also be mentioned that in both references extensive annealing periods preceded the ion scattering experiments [70 h at 300 K (Ref. 64), and 10 h at 500 K (Ref. 65)]. According to these results, a Au-rich surface obviously is the preferred phase in the above case. Expanding on these findings one arrives at an interesting consequence for the formation of steps and terraces at the surface. In order to explain the results of a macroscopically integrating method such as ion scattering, the steps must be predominantly of bilayer height, or, in other words, terraces with a Cu plane as a surface can have only a very small area contribution. This model of the surface topography seems to be supported by atomic-resolution scanning-tunneling-microscopy (STM) exper-

iments by Niehus and Achete,[65] who reported a strong preference for bilayer steps at the $Cu_3Au(100)$ surface. The average lateral extension of the terraces was of the order of several 100 Å, being a relatively small value. The surface of the individual terraces exhibited a regular corrugation, which is interpreted as being due to an ordered array of copper and gold atoms. It is not yet clear from this study, however, whether or not the bilayer steps may consist of two closely spaced monolayer steps, which should be energetically more favorable than a true bilayer step. Since our own experimental facility does not yet include scanning tunneling microscopy, we can only assume that the findings in Ref. 65 also apply to our own sample.[66] It is important to note that the behavior of the $Cu_3Au(100)$ surface is in strong contrast to Cu(100), in which case monolayer steps are bounding adjacent terraces. The copper substrate also showed a tendency to form step bands by agglomeration of monolayer steps, yielding atomically flat terraces with lateral dimensions of several thousand Å,[37] and they are, as such, about a factor of 10 larger than those observed in Ref. 65. It must be expected that the particular topography of the $Cu_3Au(100)$ surface discussed above will have a significant influence on the growth of the iron films.

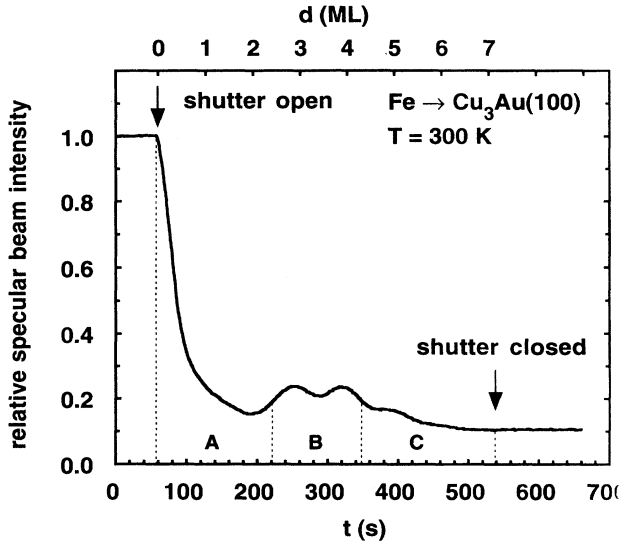

FIG. 1. Intensity variation of the MEED specular beam during the growth of $Fe/Cu_3Au(001)$ at room temperature. The labels A, B, and C distinguish regions of different growth behavior.

IV. EPITAXIAL GROWTH OF THE IRON FILMS

Prior to deposition of each film, the $Cu_3Au(001)$ substrate was briefly cleaned by Ar^+ ion bombardment, annealed to 900 K for 2 min and finally tempered for 30 min at ~600 K to restore the chemical order. During growth the substrate was held at 300 K to minimize interdiffusion and to make contact to similar work on Fe/Cu(100). The growth temperature was carefully controlled by cooling the manipulator with liquid nitrogen, while reproducibly heating the sample up to the desired temperature within a range of ±5 K. The deposition rate was approximately 1 atomic layer per minute. Figure 1 shows a typical evolution of the MEED specular beam intensity with the deposition time $I(t)$. The primary electron energy in this example was set to 2 keV. Two features in this graph point out very clearly that the growth does not proceed in a trivial manner. First, after starting the deposition the specular beam intensity drops quickly down to less than 10% of its initial value. Such a behavior is usually interpreted as a strong increase in surface roughness, corresponding to a high number of nucleation sites and small islands of the growing film. Secondly, the onset of regularly spaced oscillations is significantly delayed. The amplitude of the oscillations is small, as is the average intensity, and the oscillations are damped out very quickly. These findings indicate that the inital state of the growth certainly does not follow a perfect layer-by-layer mode. Usually the maxima in the $I(t)$ curves are interpreted as the completion of the individual monolayers.[67] This point of view is only justified, however, for a reasonably pronounced layer-by-layer growth, where the diffracted intensity is determined predominantly by the roughness of one layer. This has been found, for example, in Co/Cu (100).[68] In systems in which several layers grow more or less simultaneously (multilayer growth mode), a maximum in the diffracted intensity indicates only a minimum in the surface roughness averaged over all uncompleted layers. Such a growth mode is compatible with the initial variation of the MEED specular intensity up to the first relative maximum (region A). We will discuss this in more detail below. After this maximum, we obviously have a change in the growth mode, as periodic intensity oscillations indicative of a quasi-layer-by-layer growth start to appear (regions B and C). After two maxima of about equal height, these oscillations are quickly damped out, and the average specular intensity drops again (region C). In terms of the period of these oscillations, the first relative intensity maximum corresponds to a deposition of about three monolayers (ML) equivalent. This means that the multilayer growth in region A is essentially limited to the first three layers.

Despite this complication in the initial build up of the layers, the films are structurally well ordered. The LEED pattern in the whole thickness range up to 7 ML exhibits a $p(1\times1)$ symmetry, with the spots slightly broadened and a higher background as compared to the clean substrate surface up to coverages of about 4 ML. This confirms the pseudomorphic growth of Fe on $Cu_3Au(100)$ already reported by others.[34,35] At coverages above 4 ML the quality of the LEED pattern in terms of spot-to-background ratio deteriorates increasingly, indicating higher surface roughness or larger structural disorder. The LEED reflexes of the Fe film are found to fall on top of the $p(1\times1)$ pattern seen on the chemically disordered $Cu_3Au(001)$ surface. We therefore conclude that the in-plane lattice spacing of the Fe films is very close to that of the substrate lattice. The vertical interplanar distance in the Fe films can only be deduced from a quantitative interpretation of LEED $I(V)$ curves. Rochow *et al.*[34] give a kinematical analysis for the {00} beam and

find a lattice parameter of $a_0 = 3.75$ Å for a 5-ML film. Moreover, for the $I(V)$ curves of the clean substrate and the 5-ML film, very similar shapes are reported (Fig. 2 in Ref. 34). On the one hand, these observations suggest a strong similarity in the lattices, pointing towards a fcc-type structure of the Fe films. On the other hand, considering the relatively large mismatch of the γ-Fe bulk lattice constant, one should expect the films to be subject to a tetragonal distortion of the cubic symmetry in order to at least partly accommodate the strain. This is an important issue, since both the strain in the lattice and the deviation from the cubic symmetry may affect the magnetic anisotropy. In order to decide about the question of eventual lattice distortions, precise $I(V)$ measurements of the higher-order beams and appropriate multiple-scattering calculations are needed. We are well aware of the fact that a small tetragonal distortion in the films cannot be excluded in the present situation. For reasons of simplicity, we therefore refer to the films as fcc structured in the following.

The change from multilayer to layer-by-layer growth is an interesting feature of the Fe/Cu_3Au(100) system. It raises the question to what extent the observed behavior may be induced by the specific properties of the substrate surface. These are, as we recall from above, (i) a mixed Cu-Au surface layer and (ii) the possible presence of bilayer steps. For the completeness of the argument it is useful to briefly review some results from previous work on Fe/Cu(100) and Co/Cu(100). In both cases it is well known that the growth of the first two monolayers differs from that of the subsequent ones. In the Co/Cu(100) system this merely causes a less pronounced first relative maximum in the MEED intensity oscillations.[38] STM investigations revealed that to be a consequence of the second layer forming with the first one still being uncompleted.[69] The strong thickness dependence of the Curie temperature observed in the monolayer regime is partially attributed to this deviation from the ideal layer-by-layer growth.[70] In the case of Fe/Cu(100) the first maximum is found to be completely absent.[13] The situation in this system is more complicated, as some of the recent studies indicate that besides the film topography also a roughening of the Fe-Cu interface might have to be taken into account.[25,71] The driving force of the interface roughening, which is reported to occur already at room temperature via substitution of first-layer substrate atoms by Fe adatoms, is mainly seen in the difference in the surface free energies of Fe and Cu. The "missing" first intensity maximum is attributed to a roughening of the surface topography in the initial state of growth followed by a multilayer growth of the first two layers.[28] Note that due to the incorporation of Cu into the first monolayer at least 2 ML of iron are needed to completely cover the exposed Cu atoms and enable a Fe/Fe homoepitaxy. Being thermally activated, the interface roughening process will strongly depend on the sample temperature. A careful control of this parameter in the experiment is therefore mandatory, and its neglect in some cases may explain why the occurrence of interface roughening in Fe/Cu(100) is still a matter of dispute.[72]

How do the findings in the iron-copper system relate to the Cu_3Au substrate? A comparison of the surface free energies for polycrystalline materials indicates the surface free energy γ_S of gold to be even lower than that of copper (Ref. 73 gives values of γ_S=1.9 J/m^2 for copper, γ_S=1.6 J/m^2 for gold, and γ_S=2.9 J/m^2 for iron). Expanding on the findings in the Fe/Cu system, it is therefore reasonable to assume for the alloy surface with a $Au_{0.5}Cu_{0.5}$ composition a similar affinity to interface roughening. It is unlikely that this process extends into deeper layers of the substrate or involves a significantly larger mass transport compared to pure Cu, as this would clearly show up as a systematic deviation in the Auger uptake curves. The fact that we have an alloy as substrate material introduces another complication. Although the difference in the surface free energies of copper and gold is small, it cannot be ignored that both constituents play nonequivalent roles in a possible interface roughening process. Recent investigations of the system Fe/Au(100) revealed that the iron/gold interface is subject to a similar roughening by atomic place exchange between the Au surface layer and the first two iron layers.[74–76] Furthermore, a certain amount of gold tends to float on the surface of the growing film in the form of monolayer patches, thereby presumably acting as a surfactant. Whereas the fact of interface roughening and gold surface segregation in the monolayer regime of the iron films is commonly accepted, the actual amount of gold on the surface and its final position in the limit of thick films is still a matter of dispute. Some authors find the Au patches to be buried by Fe adatoms;[75] others observe spurious amounts of gold even on the surface of iron films several tens of monolayers thick.[76] These results suggest that with respect to iron films gold has a stronger tendency to segregate than copper. The alloy surface contains a 50% fraction of Au in the first layer; a certain influence on the growth of the iron films may thus be expected. The authors of Ref. 34 interpret some weak features in their photoemission spectra as being due to a very limited amount of Au either incorporated in the film or even floating out on its surface. Keeping in mind the importance of the growth temperature emphasized above this point certainly needs further experimental clarification, for example, by a systematic variation of the growth temperature.

Regarding the MEED oscillations, the results of Chambliss and Johnson[28] show that minuscule changes in the surface topography during growth are sufficient to introduce pronounced effects in the intensity variation of a diffracted electron beam. In the case of Fe on a Cu(100) substrate, such a change in topography occurs once the size of the first-layer islands is large enough for the onset of a significant second-layer island contribution. This happens at a total coverage of approximately 0.7 ML.[28] The process is not a literal bilayer growth proposed by others,[31] since there is no significant formation of bilayer islands at the very beginning of the deposition. In order to explain the findings in MEED on Fe/Cu_3Au(100) we are led to the conclusion that the first three Fe layers are involved in a similar process, as described above. In general, this process would be termed a multilayer growth mode in the following sense: the second layer

starts to grow after a critical coverage in the first layer has been reached, and the third-layer islands form before the second—and maybe even the first—layer is completely closed. The surface roughness as the determining quantity is therefore distributed over three layers. Several mechanisms could act as driving forces for this particular growth mode. There are, first of all, the thermodynamical properties of the alloy surface. Due to the admixture of gold, the surface free energy of the alloy should be smaller than that of pure Cu. Because of its higher surface free energy, iron does not wet the substrate surface, which may cause a formation of three-dimensional iron clusters instead of a flat continuous film. This is closely connected to the problem of a possible interface roughening and Cu and/or Au segregation. Second, the lattice mismatch between fcc Fe and Cu_3Au causes strain, which can be more easily accommodated by the formation of small islands. Third, there is still the unknown influence of the bilayer steps. These bilayer steps certainly play a role as diffusion barriers and nucleation sites. In the limit of large terraces, as they have been found on well-prepared Cu surfaces; however, their influence should be negligible to a first-order approximation. Finally, there may be a difference in growth on a copper terminated terrace and a terrace with a gold-rich surface termination. A further investigation of the influence of these mechanisms must be based on microscopic analyses of the growth dynamics and requires the use of scanning-tunneling microscopy. This was beyond the scope of the present approach and is the topic of an ongoing study.[77]

The presence of intensity oscillations in regions B and C indicates the onset of a quasi-layer-by-layer growth mode. As has been already mentioned, however, the films accumulate structural defects, causing the MEED intensity oscillations to be damped out after approximately 6–7 ML. A closer inspection of Fig. 1 reveals more details about this process. The intensity maxima corresponding to the growth of the third and fourth layer are about the same height and therefore reflect two equivalent states of the surface with respect to the roughness. During the growth of the fifth and the subsequent layers the intensity oscillations become continuously weaker and the average intensity is reduced, finally assuming an almost constant value at about 7 ML (region C). The disappearance of the MEED intensity oscillations is accompanied by a severe deterioration of the LEED pattern. Preliminary LEED $I(V)$ investigations on these films indicate the presence of iron in the bcc lattice structure.[77] Similar observations have been made in Ref. 34 but for much thicker films ($\sim$250 Å). We therefore tentatively attribute the findings in the electron diffraction experiments to a transformation from the fcc to the bcc structural phase. Given the structural similarities of thicker fcc Fe layers grown on Cu(100) and Cu_3Au(100), the structural transformation presumably follows a similar path, as has been found in Fe/Cu(100).[21,78] We note that the more gradual behavior found in the present system is in contrast to Fe/Cu(100), where a sudden disruption of the MEED intensity oscillations after 11 ML was observed.[13] From the above discussion of the MEED data, we conclude that the accumulation of defects in the film increases significantly with the growth of the fifth monolayer. We cannot determine the exact nature of these defects, but we believe that they consist at least in part of structurally transformed areas in the film.

In view of the relatively complicated growth mode, some comments on the thickness calibration must be made. We used essentially three independent indicators for this purpose: (i) MEED intensity oscillations, (ii) measurements of the flux of iron atoms at the evaporator, and (iii) Auger signal vs deposition time uptake curves. The results from the MEED analysis were in a first step correlated with the readings of the flux monitor. The only assumptions that entered the analysis were those of a monolayer separation of the intensity maxima observed above 3-ML film thickness and a constant sticking probability. This procedure yielded a thickness calibration in terms of monolayers per unit deposition time. The amount of deposited material necessary to reach the first relative intensity maximum was thus determined to be the equivalent of 3 ML. In a second step we evaluated the ratio between the AES signals from Fe (651 eV) and from Cu (920 eV) as a function of coverage given by the first calibration.[35] The resulting thickness dependence was compared to a theoretical curve of the Auger signal vs coverage dependence by means of a least-squares fit with the inelastic mean free paths as fit parameters. The values obtained from this fit procedure were found to be smaller than the tabulated ones ($\lambda_{651} \approx 9$ Å and $\lambda_{920} \approx 11$ Å), but agreed nicely with the experiences made in the Co/Cu system. The growth model leading to the calculated Auger signal vs coverage dependence included a multilayer growth mode limited to three monolayers as described above, followed by an ideal layer-by-layer growth. Whereas each of the individual approaches (ii) and (iii) may not be reliable enough, the results from all three methods gives us confidence in our coverage calibration. This consistency also rules out the possibility of a true bilayer growth, as one might be tempted to infer from the presence of bilayer step heights on the clean surface.

V. MAGNETIC BEHAVIOR OF $Fe/Cu_3Au(100)$

A. Spin reorientation

The measurements of the polar and longitudinal magneto-optical Kerr effect (MOKE) were performed between 350 and 160 K. As the interest is focused primarily on the perpendicular anisotropy, only films with thicknesses less than 8 ML were investigated. Figure 2 contains a compilation of hysteresis loops in the polar MOKE recorded at 160 K for various Fe coverages. This compilation clearly shows the strong variation of the loop shapes and the magnetic key parameters, such as remanence, coercive field, and saturation magnetization, over the thickness range investigated. At a coverage of 1.7 ML we do not see any indication of a ferromagnetic response, neither in the polar nor the longitudinal geometry. This implies the absence of a long-range ferromagnetic order. A Curie temperature, which is usually considerably re-

duced for very thin films compared to the bulk value, is consistent with findings in other thin film systems. Nevertheless, the Kerr signal is not independent of the applied field, but shows a weak linear variation. This suggests that the Curie temperature T_C at this coverage is only slightly lower than the measuring temperature, and the signal is due to the paramagnetic response of the system close to T_C.

This interpretation is further backed by the results of the 2.1-ML film, where we evidence the presence of a perpendicular component of the magnetization. The remanence is still very small and a temperature scan (see below) reveals that T_C is below 200 K. The loop becomes more pronounced for the coverage of 2.2 ML.

At 2.5 ML we finally observe an almost rectangular loop with slightly rounded edges. This behavior is found for all coverages between 2.5 and 3 ML. We notice, however, a sudden drop in the coercive field between 2.7 and 2.9 ML. The hysteresis loops between 2.5 and 3 ML are characterized by a large remanence, indicating an easy direction of the magnetization perpendicular to the film plane.[57] The slopes of the loops are not vertical, but inclined, which is interpreted by the formation and motion of domains during magnetization reversal.[12,59,79] The presence of domains is not surprising, and conditions for their presence in thin films have been discussed by Yafet and Gyorgy[80] and Czeck and Villain.[46]

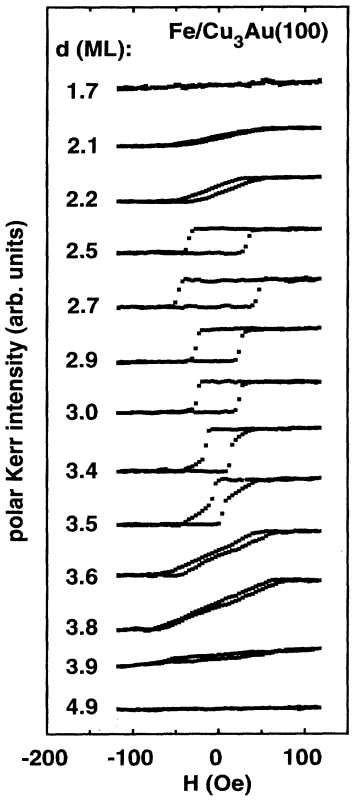

FIG. 2. Hysteresis loops in the polar Kerr effect for various Fe coverages taken at T=160 K. The film thickness ranges from 1.7 to 4.9 ML.

Above 3 ML the hysteresis loops again undergo marked changes. They develop a sheared "hourglass" shape up to about 3.5 ML. This particular form of the hysteresis reflects a complex process of magnetization reversal, and one might be tempted to relate it to the presence of an easy axis, which is inclined to the surface normal. The thickness of 3.5 ML is in fact close to the coverage at which the authors of Ref. 34 start to see an in-plane component of the magnetization. Unfortunately, details of the magnetization reversal process are, in general, very difficult to extract from an hysteresis loop, which represents a kind of integral measure.[57,81] We therefore have to consider several aspects, which eventually lead to the same form of hysteresis loops. In the most straightforward approach, one could think of the loops as composed from contributions of two independent mechanisms of moment reversal. The first contribution is due to the perpendicular anisotropy, causing the high remanence and initial steep slope of the loops after field reversal. The second contribution is responsible for the round off of the loops and may be due to an easy axis, which is no longer aligned with the surface normal.[62] A coexistence of two different easy axes resulting in a superposition of the individual magnetic signals in the measuring procedure could point towards an inhomogeneity in coverage. Parts of the sample with a lower coverage still have the easy axis normal to the surface, whereas in parts with a somewhat higher coverage a different easy axis dominates. A small difference in coverage across the total lateral dimension of the sample ($\sim$10 mm) cannot be excluded. The probing laser spot, however, is less than 1 mm in diameter in the polar geometry. The hypothesis of macroscopic inhomogeneities must therefore be dismissed as the reason for the shape of the hysteresis loops. Microscopic inhomogeneities, i.e., islands of different height, in contrast, should not be able to develop an individual magnetic behavior, because of a strong mutual ferromagnetic coupling. We thus conclude that the loops at 3.4 and 3.5 ML represent the intrinsic magnetic response of the system. If this response involves an easy axis inclined to the surface normal, however, the inclination can only be very small. We extract this information from MOKE measurements in the longitudinal geometry, which show no in-plane magnetic signal below 3.8 ML above the noise level (Fig. 3). We also note that any rotation of the easy axis away from the surface normal should lead to a formation of domains as we have a fourfold symmetric surface. This means there are four equivalent in-plane directions into which the easy axis can possibly rotate. We recall in this context that the spin reorientation transition in Fe/Cu(001) was seen to start by the formation of stripe domains.[16] The quintessence of the above discussion is therefore that the transition from a rectangular to an hourglass shape in the hysteresis loops indicates the onset of a spin reorientation, but is related rather to the formation of domains than to a sizeable rotation of the easy axis. This conclusion is supported by recent theoretical and experimental investigations on perpendicularly magnetized TbFeCo films, which exhibit a similar change in the loop shape as a function of temperature.[82] Computer simulations showed a distinct connection between

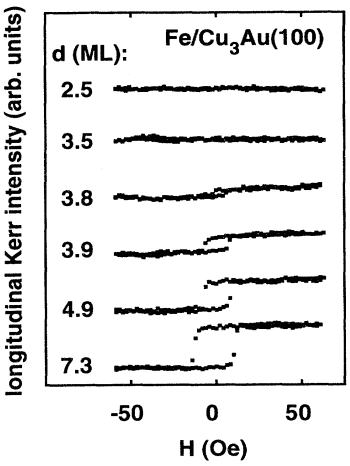

FIG. 3. Hysteresis loops in the longitudinal Kerr effect for selected coverages in the range from 2.5 to 7.3 ML. Sample temperature during the measurement was T=160 K.

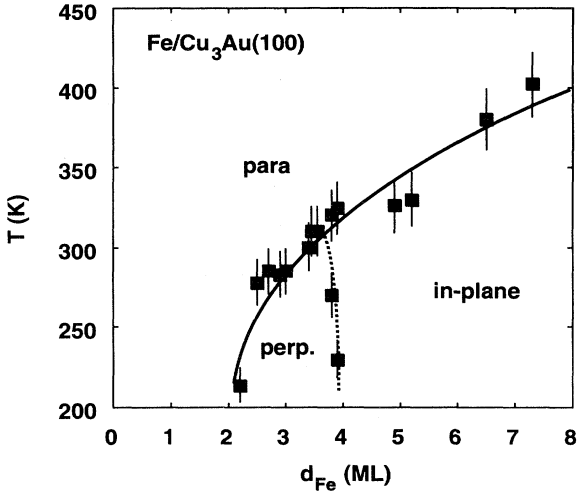

FIG. 4. Magnetic phase diagram of $Fe/Cu_3Au(001)$. The solid line gives the Curie temperature of the films, whereas the broken line separates the regimes of in-plane and perpendicular magnetization. Both lines serve as a guide to the eye.

the loop shape and the corresponding magnetic domain patterns. Whereas the rectangular hysteresis loops have been related to a uniform domain growth, the sheared loops turned out to be a consequence of fractal domain growth during magnetization reversal. The reason for the formation of fractal domains is traced back to differences in the activation energies for domain nucleation and domain-wall motion. As the domain-wall motion is affected by the defects in the film and therefore by morphology, this finding might point towards an interesting link between surface roughness and magnetic domain structure. It would certainly be interesting to know more about the process of magnetization reversal and the underlying domain structure in our own films. These aspects must be left to domain imaging experiments.[83,84]

Above the coverage of 3.5 ML the magnetic response takes more and more the form of a hard axis loop. This interpretation is confirmed by results from the longitudinal MOKE (Fig. 4), which reveal the onset of a magnetic signal and hysteresis loop between 3.5 and 3.8 ML. Parallel to the development of the in-plane hysteresis the remanence in the out-of-plane loops decreases, and the field required to reach magnetic saturation increases. At about 5 ML the coercive field of the films is obviously too high for the magnetization to be forced perpendicular to the surface. Instead we observe a pronounced rectangular hysteresis loop in the in-plane magnetic component. Both the in-plane Kerr signal and coercive field increase with the coverage up to 7 ML.

These findings indicate that the system exhibits a continuous change of the magnetization direction rather than a sudden flip at a given coverage. In other words, the transition from perpendicular easy axis to in-plane easy axis behavior comes progressively in the coverage range between 3.5 and 4 ML with an increasing angle between the macroscopic magnetization and the surface normal. This angle is given by the minimum anisotropy energy.[57] Accordingly we find two critical values for the thickness. Below $t_{c,1} \leq 3.5$ ML the magnetization direction is determined by the perpendicular anisotropy. Above $t_{c,2} \geq 4$ ML the magnetization lies in-plane, presumably due to a dominant contribution of the shape anisotropy. This behavior has exactly been addressed in a recent paper by Fritzsche *et al.*,[85] who attributed it to the presence of fourth-order contributions in the magnetic surface anisotropy. We recall that both the surface anisotropy in the Néel model and the shape anisotropy are usually considered in the quadratic approximation:[86,87]

$$E_{\mathrm{MSA}} = K_S \cos^2 \vartheta, \tag{5.1}$$

$$E_S = J_S^2 / 2\mu_0 t \cos^2 \vartheta. \tag{5.2}$$

E_{MSA} and E_S are the contributions of the magnetic surface anisotropy and shape anisotropy, respectively, to the total free-energy density per unit area. K_S denotes the surface anisotropy constant, J_S the saturation magnetization, $\mu_0 = 4\pi \times 10^{-7}\ \mathrm{V\,s\,A^{-1}\,m^{-1}}$, t the film thickness, and ϑ the angle between the magnetization and the surface normal. In the notation of Ref. 85, K_S<0 corresponds to a perpendicular anisotropy. Higher-order terms in the surface anisotropy are often considered of minor importance and thus neglected. In the particular case of a compensation of shape and surface anisotropy, however, these higher-order terms may become important and eventually dominate the magnetic behavior of the system in the reorientation regime. It must be pointed out that this inclusion of higher-order terms in the discussion is first of all a phenomenological approach. The physical mechanisms leading to these higher-order contributions still remain to be identified.

Apart from higher-order terms in the surface anisotropy, we may have a contribution from the bulk magnetocrystalline anisotropy. Even in films only a few monolayers thick this anisotropy is strong enough to define pronounced in-plane easy axes, as has been seen in

fcc-Co/Cu(001).[88,89] For this reason we expect that any canting of the magnetization during a continuous reorientation transition should be accompanied by the formation of domains. Whether these are stripe domains as observed in Fe/Cu(001) can, of course, not be extracted from our MOKE measurements. In any case, the explicit type of magnetic domains need not to be the same as in Ref. 16, because the growth conditions are different, and therefore very likely also the morphology. Within each domain, the magnetization can then rotate into the film plane with increasing coverage. Once being in-plane, the behavior of the magnetization and the domain pattern should be entirely governed by the higher-order terms in the anisotropy.

B. Magnetic phase diagram and onset of magnetic order

The magnetic anisotropy is not only dependent on film thickness but varies also with temperature.[59] Figure 4 shows a phase diagram giving the magnetic order and the spatial orientation of the magnetization as a function of thickness and temperature. The general structure of this phase diagram resembles that of Fe/Cu(001), but distinct differences are found in the details. There are two main regions which correspond to a paramagnetic and an ordered magnetic phase separated by a continuous line marking the Curie temperature $T_C(t)$ as a function of Fe coverage. The phase of magnetic order is subdivided into regions of out-of-plane and in-plane magnetization. The dashed line gives the limit of the perpendicular anisotropy area and is called the reorientational temperature T_R.[41,48,59] The temperature T_R decreases with the film thickness, just as for Fe/Cu(100).[11] We also notice that the transition occurs on a relatively large temperature width ΔT. In the film of 3.8 ML (Fig. 5), for example, both an in-plane and a perpendicular component of the magnetization with varying strength are observed between 160- and 260-K sample temperature. We therefore deduce a value for ΔT of at least 100 K for this film.

Two further findings concern the behavior of the Curie temperature $T_C(t)$ in Fig. 4. First of all, we notice a sharp decrease of the Curie temperature as soon as the coverage reaches values below 2.5 ML. In fact, we can linearly extrapolate this behavior to T=0 K in order to obtain the minimum thickness required for ferromagnetic order. This extrapolation may be only a very crude approximation to the actual situation, but we are only interested in trends at this point. The procedure yields a minimum thickness of $t_m(T = 0\ \mathrm{K}) \approx 1$ ML. A delayed onset of the ferromagnetic order can have several reasons. Among them are the reduction of the magnetic moment due to electronic hybridization with the substrate, and the question of structural and magnetic percolation. We must emphasize that this result by itself does not yet mean that iron atoms at the Fe-Cu_3Au interface in thicker films do not contribute to the ferromagnetism of the system. This information, however, emerges from the thickness dependence of the Kerr signal at maximum applied field $I_{K,S}(t)$ [Fig. 6(b)], which is proportional to the saturation magnetization $M_S(t)$ of the films below $T_C(t)$.[90] A linear extrapolation to vanishing saturation $I_{K,S} = 0$ does not go through zero, but yields a residual value of the order of 0.5 ML. This suggests that a submonolayer fraction of the iron film does not contribute to the observed ferromagnetism of the system. Whether

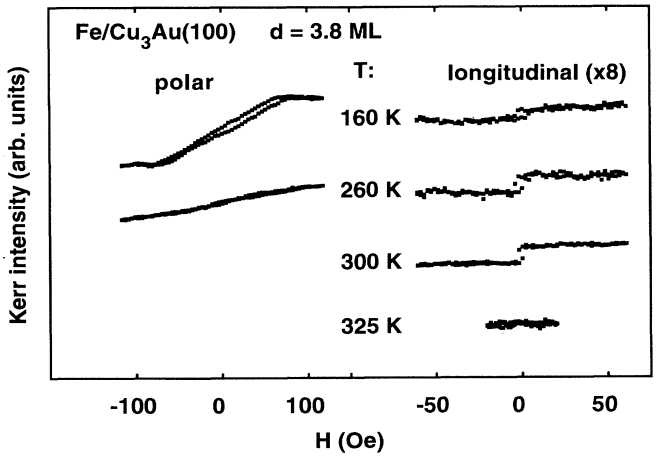

FIG. 5. Temperature dependence of the hysteresis loops in the longitudinal and polar Kerr geometry for a 3.8-ML iron film.

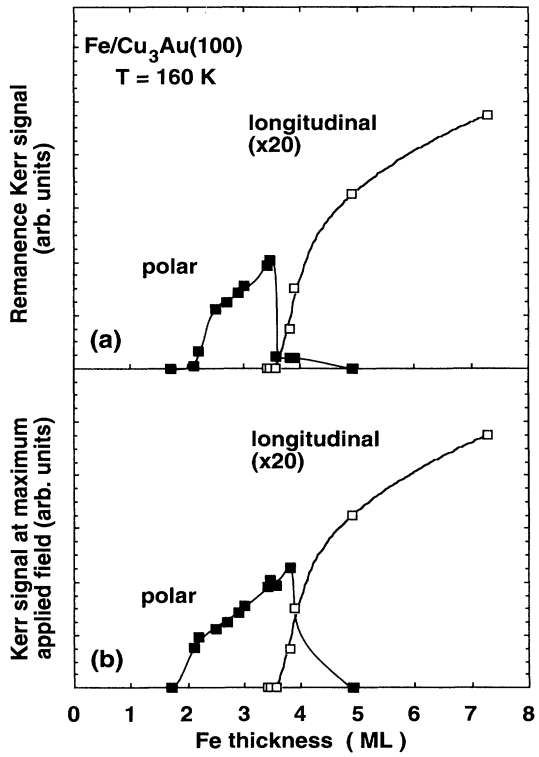

FIG. 6. Thickness dependence of the polar (filled squares) and longitudinal Kerr signal (open squares) at remanence (a) and maximum applied field (b) measured at T=160 K. Lines serve as a guide to the eye only.

this fraction has an antiferromagnetic character or lacks a magnetic response at all cannot be distinguished on the basis of the present data.

The second finding concerns the behavior of T_C in the vicinity of the reorientation transition. In the transition region from perpendicular to in-plane magnetization, $T_C(t)$ does not exhibit any discontinuities. Instead we observe an almost linear steady increase of T_C with the iron coverage. This is in distinct contrast to the Fe/Cu(001) system in which strong variations of the Curie temperature due to the formation of antiferromagnetic underlayers have been found.[13] Expanding on the Mermin-Wagner theorem, recent theoretical work explored the relation between magnetic anisotropy and ferromagnetic ordering temperature.[41,42,44] The calculations predict significantly larger T_C values for a magnetization perpendicular to the surface than for the in-plane magnetization. These results imply a reduction of the Curie temperature when crossing the reorientation regime. This reduction, however, has not yet been experimentally observed, and there are also no indications for it in our own data.

VI. STRUCTURE AND MAGNETISM

We will now relate the magnetic properties described in the preceding paragraph to the film structure and morphology. For this purpose the discussion is divided into four sections, covering (i) the initial state of growth, (ii) the thickness range of perpendicular magnetization, (iii) the spin reorientation regime, and (iv) the regime of in-plane magnetization.

Starting with the initial state of growth, we recall that the multilayer growth mode up to the third layer causes an extremely high surface roughness, since three different height levels are growing simultaneously. At a coverage of the equivalent of 1 ML the film may therefore not have reached its percolation limit. In Fe/Cu(001) the percolation limit for the first layer was found to be of the order of 0.7-ML total coverage.[28] The roughness at this coverage, however, is essentially confined to two layers. Translating this result to the situation in $Fe/Cu_3Au(001)$ requires the same amout of iron to be distributed over three layers, thus leaving less material in the first layer than in Fe/Cu(001). In this case the percolation of the first layer will occur at a somewhat higher total coverage, which can explain the delayed onset of ferromagnetic order and the very steep increase in the Curie temperature below 2-ML total coverage. A further aspect needs to be considered in the view of a possible ferromagnetically inactive interface contribution of iron. It has already been shown for Co monolayers on Cu(001) that an additional cover layer of copper reduced the Curie temperature.[37] This is attributed to a hybridization of the electronic states at the Co/Cu interfaces and will certainly be valid for a Fe/Cu or Fe/Cu_3Au interface as well. This argument gains even more weight in the context of a possible interface roughening during the growth of the Fe films. Fe atoms, which are incorporated in the Cu surface will experience a higher degree of electronic hybridization than those located in the first iron layer. One must therefore expect that the reduction of the magnetic moment and magnetic order is enhanced by a rough interface. The layers that are affected by this process will therefore only partially contribute to the total magnetic response of the system. In order to decide which of these two effects is finally responsible for the magnetic behavior in the monolayer regime detailed morphology investigations in the coverage regime up to 2 ML are needed. Furthermore, the Kerr effect experiments have to be extended to lower temperatures to permit a more precise determination of the critical thickness for the onset of magnetic ordering.

In the thickness range between 2 and 4 ML we observe the magnetization to be oriented normal to the surface. The Curie temperature of the perpendicularly magnetized state reaches a maximum slightly above room temperature at about 3.5-ML coverage (Fig. 4). The reduction of the coercive field upon the completion of the third monolayer mentioned above can be understood in terms of the roughness of the growing film. The defects in the film (holes due to uncompleted underlying layers) act as pinning sites for the magnetic domains and therefore hinder the motion of the domain walls. Consequently a higher external field is required to overcome the coercive force and to drive the domain walls until the magnetization reversal is completed. With the completion of the third monolayer the surface roughness is considerably reduced, as reflected in the decrease of the coercive field.

According to the results of the electron diffraction experiments the spin-reorientation takes place in a thickness regime in which effects due to the structural transformation can still be neglected. This is an important finding as it marks one of the essential differences between the Fe/Cu(001) and $Fe/Cu_3Au(001)$ system. We can therefore expect that the spin reorientation observed in $Fe/Cu_3Au(001)$ indeed reflects the competition between the different contributions to the magnetic anisotropy. The shape anisotropy due to the demagnetizing field increases with the coverage and overcompensates the surface anisotropy, thus turning the magnetization into the film plane. The surface anisotropy is, of course, the sum of the anisotropies of the Fe/vacuum and Fe/Cu_3Au interfaces. At a coverage of 4 ML, the magnetization has been rotated entirely in plane. If we know the numerical value of the shape anisotropy under these conditions, we can estimate the surface anisotropy. It is instructive to compare this number to corresponding results of other iron thin-film systems. In bcc Fe (110)/Cr(110) the critical thickness is determined to about 2.5 ML at room temperature.[85] The values for bcc Fe(001)/Ag(001) range between 4 and 7 ML depending on the temperature.[58] There are no experimental data on the magnetic moment or saturation magnetization of fcc iron in the strained lattice on $Cu_3Au(001)$. The theoretical prediction for the high-spin magnetic state of $\mu_{HS} = 2.3\mu_B$/atom (Refs. 7, 8) is close to the bulk magnetic moment of bcc iron ($2.2\mu_B$/atom).[91] Investigations with conversion electron Mößbauer spectroscopy on $Fe/Cu_3Au(001)$ determined a magnetic hyperfine field[92] about 3% larger than in bulk bcc iron. This suggests

that the magnetic moment in the high-spin state may indeed be slightly enhanced over that of bcc iron, but experimental values are not yet available. We therefore use the bulk bcc value as a basis for a conservative estimate of the lower limit for the anisotropy. From the comparably lower value of the critical thickness, we can directly conclude that the perpendicular anisotropy in fcc $Fe/Cu_3Au(001)$ is significantly weaker than the one in bcc Fe/Ag(001). In the reorientation regime $E_S \approx E_{MSA}$ (neglecting the higher-order anisotropy contributions), and Eq. (2) can be substituted into Eq. (1) in order to extract a numerical value for the anisotropy constant K_S. Using for the saturation magnetization at T=160 K a value of $J_S = 2.2$ T (Ref. 91), we obtain a lower limit for the surface anisotropy of $K_S = -1.4$ mJ/m^2. This is of the same order as the value determined for Fe/Cr(110) (Ref. 85) and compares well with the surface anisotropies found in the Fe/Cu(001) system.[93]

Compared to $Fe/Cu_3Au(001)$, the spin reorientation regime in room-temperature-grown Fe/Cu(001) is found at much higher coverages, namely, around 11 ML.[13] This is, however, not a reasonable comparison, as the antiferromagnetic sublayers reported to form in these iron films above 4–5 ML reduce the total magnetization of the film. In this case the demagnetizing field is generated only by the ferromagnetic surface layer, plus a contribution from an odd number of antiferromagnetic layers, if a layer antiferromagnetism is assumed. Recent experiments indeed found an indication of these antiferromagnetic contributions.[19] A ferromagnetic contribution from the entire film is only observed at coverages up to about 4–5 ML,[13,19] which is still measurably higher than the value determined for $Fe/Cu_3Au(001)$. The first idea that comes to mind is that this difference might be due to a smaller shape anisotropy in Fe/Cu(001) caused by a reduced magnetic moment. Although this argument would be along the lines of the theoretically predicted magnetic moments, it should be backed by experimental evidence. The difference of 3% found in the magnetic hyperfine fields for the two systems[92] suggests a higher magnetic moment for $Fe/Cu_3Au(001)$, but the correlation between magnetic moment and hyperfine field is not straightforward. There is a second possibility to explain the different magnetic response of the Fe films on the two substrates. The perpendicular surface anisotropy in our system is either reduced by intrinsic mechanisms or by competition with the bulk anisotropy contributions. The latter can have various origins, the first one associated with the lattice mismatch. A tetragonal distortion of the cubic bulk symmetry could lead to the appearance of second-order terms in the bulk magnetocrystalline anisotropy energy. Under these conditions the effect of the broken symmetry at the surface may not be as pronounced as for a pure cubic phase, presumably leading to a smaller surface anisotropy. In the following we will examine some possible physical mechanisms that can give rise to extra magnetic anisotropies. As pointed out by Bruno,[61] the magnetic behavior of ultrathin epitaxial films may be decidedly affected by specific structural and morphological aspects, namely, the surface roughness and magnetostriction.

A comparative study of the surface roughness of the two types of iron films on Cu(001) and $Cu_3Au(001)$ still needs to be done. As a first step, we compare in Fig. 7 the content of Fig. 1 to the MEED intensity variation $I_M(t)$ during the growth of 6-ML Fe on Cu(001). Special care has been taken to obtain the same experimental parameters in order to permit a direct comparison of the two curves. Still, the amplitude of the oscillations depends very sensitively on the diffraction conditions and may therefore not be a reliable measure of the surface roughness. Instead we focus on the behavior of the average intensity $\overline{I_M(t)}$ as in the growth proceeds. For Fe/Cu(001) the average intensity drops down to ≈40% of the initial value, before it rises again and reaches values of ≈80% at coverages above 4 ML. In the coverage regime between 4 and ≈10 ML regular oscillations are found (see also Fig. 1 of Ref. 13). These are the same coverages for which STM investigations consistently report a layer-by-layer growth with a relatively low surface roughness.[79,97] The average MEED intensity variation for $Fe/Cu_3Au(001)$ shows marked differences in that $\overline{I_M(t)}$ decreases to minimum values of about 15%, and recovers ≈20% in the region between 3 and 4 ML. This is a strong indication that the surface roughness of Fe films on the $Cu_3Au(001)$ substrate is qualitatively higher.

These films also have a higher lattice mismatch of 4.2%, which may induce significant magnetoelastic effects. These can result in a nonzero bulk anisotropy, which partly compensates the surface anisotropy. A first quantitative description of the combined influence of surface roughness and magnetostriction within the Néel model has recently been given for stepped surfaces,[94] induced by experiments on Co and Fe films on vicinal surfaces of Cu and W, respectively.[95,96] The calculations in Ref. 94 showed the presence of distinct contributions to both volume and surface anisotropy caused by magnetostriction and surface steps. We will first concentrate on the role of magnetoelastic contributions. The analysis in

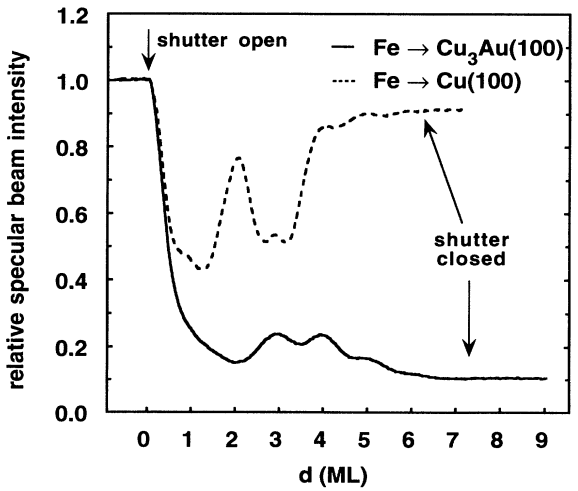

FIG. 7. Comparison of MEED intensity oscillations during the growth of Fe films on Cu(001) (broken line) and $Cu_3Au(001)$ (solid line) under identical experimental conditions.

Ref. 94 has been carried out for fcc Co films on Cu(001). Given the structural similarity of fcc Co and fcc Fe films on Cu(001) this enables us to make a relevant comparison of the two cases. The lattice mismatch for fcc Co on Cu(001) is about $\Delta a \approx 1.9\%$, resulting in a tetragonally face centered (fct) structure of the films.[70] The tetragonal distortion is associated with a misfit strain in the lattice, resulting in a significant uniaxial magnetoelastic contribution to the anisotropy. This magnetostrictive anisotropy is of the order of 10^6 J/m^3 and favors an in-plane orientation of the magnetization.[94] The strength of the combined anistropies explains why fcc Co films are always in-plane magnetized regardless of the film thickness. The lattice distortion in Fe/Cu(001) is only $\Delta a \approx 1\%$, and the fact that monolayer films exhibit a perpendicular magnetization suggests a decidedly smaller magnetostrictive component in this case. The lattice mismatch for Fe/Cu_3Au(001) is much larger, i.e., $\Delta a \approx 4.2\%$, thereby causing a larger misfit strain. Since the magnetostrictive anisotropy increases with the strain and acts in the same direction as the shape anisotropy, the reorientation transition will occur at a smaller critical thickness than without a magnetoelastic contribution. Because the strain-induced anisotropy is of uniaxial character and depends on the strain distribution in the entire film, it can be regarded as one possible origin for the second-order term to the bulk anisotropy of the film mentioned above.

We now turn to the role of the surface roughness as seen in the above experiments at vicinal surfaces. Since the steps at a vicinal surface are predominantly oriented along the same spatial direction we may think of them as of an ordered kind of surface roughness. The analysis in Ref. 94 reveals a striking influence of the surface steps on the magnetic behavior of the films. Seen by their absolute value in conventional units and compared to typical bulk ($\sim 10^5$ J/m^3) and surface anisotropy energies (~ 1 mJ/m^2), the step-induced anisotropy energies seem to be relatively small ($\sim 10^{-10}$ mJ/m for atoms at step-edge sites and $\sim 10^{-11}$ mJ/m for atoms at step-corner sites[94]). If we change to atomic units, however, the impression changes markedly. A typical bulk anisotropy energy of 10^{-6} eV/atom must then be compared to values of $\sim 10^{-4}$ eV/atom and $\sim 10^{-5}$ eV/atom for the surface and step-edge anisotropy energies, respectively. This essentially means that for a surface condition with a high number of atoms in step-edge or kink positions the roughness-induced anisotropy can become an important factor. Given a thin film and a high degree of surface roughness, these step-induced anisotropy contributions may eventually dominate the magnetic behavior of the film. This behavior has exactly been observed in fcc Co/Cu(1 1 13), where the step-induced anisotropy causes the magnetization to orient itself in-plane along the step edges in films up to 17 ML thick.[94,95] This is, of course, an extreme case. The important result of theses investigations, which we can transfer to the present case, is the appearance of an additional in-plane contribution to the magnetic anisotropy due to the presence of a high density of surface steps. Moreover, due to a preferential orientation of the steps along particular crystalline lattice directions, these anisotropy contributions may no longer be uniaxial, i.e., pure second-order terms. They will therefore show up as effective higher-order terms in the total magnetic anisotropy. This way, surface roughness may be a possible source for the fourth-order anisotropy terms invoked to explain the continuous nature of the spin-reorientation transition.[85] In the fcc Fe films on Cu(001) and Cu_3Au(001) we have a more disordered kind of roughness than in the case of vicinal surfaces. If we translate the above result and compare only the two types of iron films, the higher surface roughness in the case of Fe/Cu_3Au(001) should then lead to a larger in-plane anisotropy. Again this effect would cause a shift of the spin-reorientation transition to smaller Fe coverages. We therefore tentatively attribute the observed difference in the critical thickness to an effective reduction of the perpendicular anisotropy due to a combination of higher surface roughness and stronger magnetoelastic effects.

As just discussed, the physical processes that determine the magnetic behavior in the spin reorientation regime are obviously of very complex nature. If we now concentrate on the temperature dependence of the spin reorientation, we again find large differences between Fe films grown on Cu(001) and Cu_3Au(001). From the data in Ref. 11 we estimate the temperature width of the spin reorientation, ΔT, to be around 80–90 K for Fe films on Cu(001). We define ΔT as the temperature interval in which the magnetization rotates from completely perpendicular to an entirely in-plane orientation. Furthermore, there is a smaller temperature range ΔT_R of about 20–30 K in which the magnetization in Fe/Cu(001) is essentially zero.[11] These temperature intervals ΔT and ΔT_R should not be confused, as they have entirely different physical meanings. In our system the width of the reorientation regime is somewhat larger, $\Delta T \geq 100$ K, and there are indications in the data that the magnetization may be reduced but it does not disappear during reorientation. The latter can be inferred from the presence of a nonzero remanent Kerr signal in both directions and from a comparison of the Kerr signals in remanence and maximum applied field (Fig. 6). We therefore cannot define a quantity ΔT_R in our experiments. It is instructive, however, to recall some prediction for the behavior of ΔT_R that emerges from the calculation of Erickson and Mills.[48] In their Eq. (16), ΔT_R is shown to vary with the square of the lattice parameter. Given the lattice constants of Cu and Cu_3Au, this should result in an increase of about 8%. This is, of course, based on the questionable assumption that all other quantities entering the calculation are the same for both systems. Nevertheless, instead of an enlarged temperature regime with zero magnetization, we do not observe such a regime at all.

In order to understand the physical concept behind ΔT_R, we need to look into the arguments of Ref. 48 more closely. Using a spin-wave approach the authors determined a relationship between the transition temperature T_R and the band width ΔT_R. ΔT_R is defined as the width of the region in which the long-range ferromagnetic ordering breaks down. This breakdown is essentially a consequence of the system becoming an isotropic magnetic system in the sense of the Mermin-Wagner the-

orem at T_R. Erickson and Mills estimated a ratio of $\Delta T_R/T_R \sim 5\times10^{-3}$, thus resulting in a ΔT_R of the order of 1 K for the reorientation transition experimentally observed. To make contact to the results in the Fe/Cu(001) system,[11] the authors of Ref. 48 invoked the influence of island formation in the sense of a Vollmer-Weber-type growth mode in the film. The spins within the individual islands were assumed to be strongly magnetically coupled, whereas the coupling between neighboring islands was supposed to be weak. Under these circumstances the island size instead of the lattice parameter becomes the determining quantity, and ΔT_R was predicted to reach the order of magnitude observed in the experiment. Island formation in Fe films is indeed observed for growth at cryogenic temperatures,[97] which has been employed in Ref. 11. Conversely, room-temperature-grown Fe films form consecutive layers on Cu(001),[97] Ag(001),[58] and according to our MEED results on $Cu_3Au(001)$ as well. The surface roughness that we discussed above is essentially confined to the topmost layers of the films and must not be confused with a three-dimensional island formation. For these rather flat films the above theory predicts ΔT_R to be only of the order of 1 K. This seems to be in accordance with results reported by Qiu, Pearson, and Bader[58] for the Fe/Ag(001) system.

We suggest that the absence of a ΔT_R regime with vanishing long-range magnetic order can be understood, if the continuous nature of the reorientation transition is taken into account. As we have already stated above, this behavior has been shown to be connected to the presence of higher-order terms in the magnetic anisotropy. We note that the approach of Erickson and Mills does not take into account anisotropy contributions due to magnetostriction or surface roughness, which might lead to these higher-order terms. As an important consequence, these additional anisotropy contributions remain, even when a complete compensation between shape and surface anisotropy takes place, and may then control the magnetic properties of the film. Quantitatively, these fourth-order anisotropies are significantly smaller [about a factor of 10 in Fe/Cr(110) (Ref. 85)] than, for example, the surface anisotropy. This smaller total anisotropy in the film may result in a lower Curie temperature, which eventually translates into a reduced remanent magnetization if the experiment is carried out at the same temperature. This tentative reduction of the Curie temperature around T_R still awaits experimental verification. Nevertheless, even with a reduced T_C the film never achieves magnetic isotropy required for a complete breakdown of the long-range ferromagnetic order.

We still have to discuss the origin of the gap ΔT, which shows up in the data as a regime of reduced remanent magnetization $M_R(T)$. A similar gap has been observed by Qiu, Pearson, and Bader[58] for the Fe/Ag(001) system. These authors referred to it as a "pseudo-gap" and suggested that it might be associated with the formation of a complex magnetic domain structure. In this context we recall the argument about fractal domain growth used to explain the hour-glass shape of the hysteresis loops at coverages close to the reorientation regime. Considering the influence of the various anisotropy contributions discussed above, we will indeed have to expect a complicated process of domain formation. This seems to be a likely explanation for the presence of ΔT, but it must not be an exclusive one. There may be still an additional mechanism at play involving the surface roughness. Besides the gap ΔT in the temperature dependence of the remanent magnetization $M_R(T)$, we observe a similar gap ΔT upon varying the film thickness t. The definition of Δt is analogous to that of ΔT. Why would we expect to find such a gap in the thickness dependence? In a simple picture, the two parameters T and t act on different anisotropy contributions. A small temperature variation mostly changes the surface anisotropy by means of the temperature dependence of K_S, but leaves the shape anisotropy unaffected as long as the temperature is far away from T_C. An increase of the film thickness enhances the shape anisotropy, but has no effect on K_S provided that no structural or morphological changes are encountered. The existence of such a gap Δt has been first demonstrated experimentally in Fe wedges on Ag(001) by Qiu, Pearson, and Bader,[58] who reported a width of $\Delta t \sim 2$ ML at room temperature. The corresponding value in $Fe/Cu_3Au(001)$ at T=160 K is found to be significantly smaller, $\Delta t \leq 1$ ML.

The width of the pseudogaps ΔT and Δt is likely to be dominated by the process of domain formation. This can be seen by the comparison of the Kerr signal at remanence $I_{K,R}$ and at maximum applied field $I_{K,S}$ (Fig. 6). The gap appearing in $I_{K,R}$ is markedly less pronounced at maximum applied field, which orients the domains resulting in a higher Kerr signal. Whether the remaining dip in $I_{K,S}(t)$ is fully due to a reduced magnetic moment in the transition region may be doubted. We tentatively attribute it to magnetic domains, which are not yet fully aligned with the external field. This can be seen, for example, in the polar hysteresis loop of the 3.9-ML film. At maximum field we still have a nonzero slope of the $I_K(H)$ curve, indicating that magnetic saturation has not been reached. The use of a higher magnetic field may therefore well result in a disappearance of the dip. As a second competing mechanism also surface roughness can affect the width of the gap. If we consider the roughness to be confined to three layers only, a 4-ML-thick film will consist of patches with thicknesses of three, four, and five monolayers. The regions with 3-ML-film thickness have a perpendicular anisotropy, whereas regions with 4- and 5-ML thickness have an in-plane anisotropy. Since these regions are strongly ferromagnetically coupled they cannot develop an individual magnetic behavior, but result in an average magnetic response of the film. Due to this averaging the surface roughness washes out the transition from perpendicular to in-plane magnetization, which is just another way to look at a continuous spin reorientation. This suggests that a smoother film surface should be reflected in a more narrow transition region, and vice versa. We cannot go as far as to directly compare the results for Fe films on Ag(001) and $Cu_3Au(001)$ as this involves a different crystalline structure and therefore a different behavior of the magnetic anisotropies. In the bcc lattice the roughness-induced anisotropy does not have a step-edge contribution, for example.[94] A de-

tailed morphological characterization by scanning tunneling microscopy combined with high-resolution magnetic domain imaging techniques[83,84] may be able to isolate the individual physical mechanisms, which determine the magnetic response in the transition region Δt.

During the growth of the fifth monolayer the film starts to accumulate an increasing amount of defects as can be judged from the deterioration of the electron diffraction patterns. These defects are presumably due to the transformation from the fcc structure into the stable bulk bcc phase. According to the experiences with the Cu (001) substrate this process advances gradually during the growth of several layers.[78] First, only small patches in the film undergo the structural transformation. With increasing thickness these patches become larger until the entire film has been transformed. From the disappearance of the MEED and LEED patterns, and the behavior of the MEED intensity oscillations we conclude that in $Fe/Cu_3Au(001)$ this transformation process affects large parts of the film already at a coverage of 6–7 ML. This transformation introduces structural disorder in the film and thus increases the amount of pinning sites for magnetic domains. That explains why the coercive force increases with the film thickness.

VII. SUMMARY

We observed a ferromagnetic order in ultrathin fcc Fe films on $Cu_3Au(001)$ for thicknesses above 1.7 ML at 160 K. The surface anisotropy causes a perpendicular orientation of the remanent magnetization for iron coverages between 1.7 and 3.5 ML. Changes of the magnetization orientation occur both with the variation of the film thickness and the sample temperature. The magnetization is perpendicular up to 3.5 ML and in-plane for thickness higher than 4 ML at 160 K. Between 3.5 and 4 ML the angle of the magnetization with the surface normal increases progressively. This continuous reorientation transition occurs before significant structural changes in the film take place, and mainly reflects the balance between shape and surface anisotropy. The influence of the surface morphology (roughness) or magnetoelastic effects on the anisotropy balance, however, cannot be excluded. Within the magnetization reorientation regime, we find strong evidence for the formation of a complicated domain pattern. This causes the films to show a reduction, but not a total loss of the remanent magnetization. This finding and the presence of a continuous rotation are attributed to the effects of higher-order terms in the magnetic anisotropy,[85] which may be related to the influence of magnetostriction and surface roughness. Other magnetic properties as, for example, the onset of ferromagnetic order are also closely related to structural and morphological particularities of these iron films. The differences to the related system Fe/Cu (001) can be related to these particularities as well.

ACKNOWLEDGMENTS

We would like to thank J. Shen and J. Giergiel for making results of their STM investigations available to us prior to publication. We are indepted to B. Zada for her expert technical support. One of us (F.B.) would like to express his gratitude to the Alexander von Humboldt Stiftung (AvH Foundation) for supporting his stay by a research fellowship. This work was supported by the Deutsche Forschungsgemeinschaft under Grant No. Schn353-1.

* Present address: LURE Bt 209 d, Centre Universitaire Paris XI, F-91405 Orsay Cédex, France.
† Present address: Freie Universität Berlin, Fachbereich Physik, Arnimallee 14, D-14195 Berlin, Germany.
‡ Author to whom correspondence should be addressed.

[1] C.S. Wang, B.M. Klein, and H. Krakauer, Phys. Rev. Lett. **54**, 1852 (1985).
[2] C.L. Fu and A.J. Freeman, Phys. Rev. B **35**, 925 (1987).
[3] U. Gradmann and H.O. Isbert, J. Magn. Magn. Mater. **15-18**, 1109 (1980).
[4] V. Moruzzi, J.F. Janak, and A.R. Williams, *Calculated Electronic Properties of Metals* (Pergamon, New York, 1978).
[5] V.L. Moruzzi, P.M. Marcus, K. Schwarz, and P. Mohn, Phys. Rev. B **34**, 1784 (1986).
[6] O.K. Andersen, J. Madsen, U.K. Poulsen, O. Jepsen, and J. Kollar, Physica **86-88B**, 249 (1977).
[7] G.L. Krasko and G.B. Olson, Phys. Rev. B **40**, 11 536 (1989).
[8] I. Takahashi and M. Shimizu, J. Magn. Magn. Mater. **90-91**, 725 (1990).
[9] C. Paduani and E.G. da Silva, J. Magn. Magn. Mater. **134**, 161 (1994).
[10] A. Brahaus, L. Guttman, and J.S. Kosper, Phys. Rev. **127** (1962).
[11] D.P. Pappas, K.-P. Kämper, and H. Hopster, Phys. Rev. Lett. **64**, 3179 (1990).
[12] D. Pescia, M. Stampanoni, G.L. Bona, A. Vaterlaus, R.F. Willis, and F. Meier, Phys. Rev. Lett. **58**, 2126 (1987).
[13] J. Thomassen, F. May, B. Feldmann, M. Wuttig, and H. Ibach, Phys. Rev. Lett. **69**, 3831 (1992).
[14] D.P. Pappas, C.R. Brundle, and H. Hopster, Phys. Rev. B **45**, 8169 (1992).
[15] D.P. Pappas, K.-P. Kämper, B.P. Miller, H. Hopster, D.E. Fowler, C.R. Brundle, A.C. Luntz, and Z.-X. Shen, Phys. Rev. Lett. **66**, 504 (1991).
[16] R. Allenspach and A. Bischof, Phys. Rev. Lett. **69**, 3385 (1992).
[17] J.G. Tobin, G.D. Waddill, and D.P. Pappas, Phys. Rev. Lett. **68**, 3642 (1992).
[18] P. Xhonneux and E. Courtens, Phys. Rev. B **46**, 556 (1992).
[19] D. Li, M. Freitag, J. Pearson, Z.Q. Qiu, and S.D. Bader, Phys. Rev. Lett. **72**, 3112 (1994).
[20] A. Clarke, P.J. Rous, M. Arnott, G. Jennings, and R.F. Willis, Surf. Sci. **192**, L843 (1987).

[21] K. Kalki, D.D. Chambliss, K.E. Johnson, R.J. Wilson, and S. Chiang, Phys. Rev. B **48**, 18 344 (1993).
[22] J. Thomassen, B. Feldmann, and M. Wuttig, Surf. Sci. **264**, 406 (1992).
[23] P. Dastoor, M. Arnott, E.M. McCash, and W. Allison, Surf. Sci. **272**, 154 (1992).
[24] D.A. Steigerwald, I. Jacob, and W.F. Egelhoff, Jr., Surf. Sci. **202**, 472 (1988).
[25] D.A. Steigerwald and W.F. Egelhoff, Jr., Phys. Rev. Lett. **60**, 2558 (1988).
[26] S.A. Chambers, T.J. Wagener, and J.H. Weaver, Phys. Rev. B **36**, 8992 (1987).
[27] D.D. Chambliss, R.J. Wilson, and S. Chiang, J. Vac. Sci. Technol. B **10**, 1993 (1992).
[28] D.D. Chambliss and K.E. Johnson, Surf. Sci. **313**, 215 (1994).
[29] A. Brodde and H. Neddermeyer, Surf. Sci. **287/288**, 988 (1993).
[30] T. Detzel, N. Memmel, and T. Fauster, Surf. Sci. **293**, 227 (1993).
[31] H. Glatzel, T. Fauster, B.M.U. Scherzer, and V. Dose, Surf. Sci. **254**, 58 (1991).
[32] K.E. Johnson, D.D. Chambliss, R.J. Wilson, and S. Chiang, J. Vac. Sci. Technol. B **11**, 1654 (1993).
[33] *Pearson's Handbook of Crystallographic Data for Intermetallic Phases* (American Society for Metals, Cleveland, 1985).
[34] R. Rochow, C. Carbone, T. Dodt, F.P. Johnen, and E. Kisker, Phys. Rev. B **41**, 3426 (1990).
[35] S.H. Lu, J. Quinn, D. Tian, F. Jona, and P.M. Marcus, Surf. Sci. **209**, 364 (1989).
[36] M. Przybylski and U. Gradmann, Appl. Phys. **59**, 1152 (1987).
[37] C.M. Schneider, P. Bressler, P. Schuster, J.J. de Miguel, R. Miranda, and J. Kirschner, Phys. Rev. Lett. **64**, 1059 (1990).
[38] J.J. de Miguel, A. Cebollada, J.M. Gallego, S. Ferrer, R. Miranda, C.M. Schneider, P. Bressler, J. Garbe, K. Bethke, and J. Kirschner, Surf. Sci. **211-212**, 732 (1989).
[39] N.D. Mermin and H. Wagner, Phys. Rev. Lett. **17**, 1133 (1966).
[40] H. Hopster, in *Ultrathin Magnetic Structures*, edited by B. Heinrich and J.A.C. Bland (Springer-Verlag, Berlin, 1994), p. 123.
[41] D. Pescia and V.L. Pokrovsky, Phys. Rev. Lett. **65**, 2599 (1990).
[42] M. Bander and D.L. Mills, Phys. Rev. B **38**, 12 015 (1988).
[43] M.G. Tetel'man, Sov. Phys. JETP **71**, 3 (1990).
[44] R.P. Erickson and D.L. Mills, Phys. Rev. B **43**, 11 527 (1991).
[45] R.P. Erickson, Phys. Rev. B **46**, 14 194 (1992).
[46] R. Czech and J. Villain, J. Phys. Condens. Matter **1**, 619 (1989).
[47] T. Kaneyoshi, G.L. Gal, and A. Khater, Phys. Rev. B **46**, 14 190 (1992).
[48] R.P. Erickson and D.L. Mills, Phys. Rev. B **46**, 861 (1992).
[49] Y. Yafet, J. Kwo, and E.M. Gyorgy, Phys. Rev. B **33**, 6519 (1986).
[50] P. Bruno, Phys. Rev. B **43**, 615 (1991).
[51] A. Corciovei, Phys. Rev. **130**, 2223 (1963).
[52] L. Néel, J. Phys. Rad. **15**, 376 (1954).
[53] U. Gradmann, J. Magn. Magn. Mater. **54-57**, 733 (1986).
[54] J.G. Gay and R. Richter, Phys. Rev. Lett. **56**, 2728 (1987).
[55] P. Bruno, Phys. Rev. B **39**, 865 (1989).
[56] U. Gradmann, Appl. Phys. **3**, 161 (1974).
[57] C. Chappert and P. Bruno, J. Appl. Phys. **64**, 15 (1988).
[58] Z.Q. Qiu, J. Pearson, and S.D. Bader, Phys. Rev. Lett. **70**, 1006 (1993).
[59] P.J. Jensen and K.H. Bennemann, Phys. Rev. B **42**, 849 (1990).
[60] W.L. O'Brien and B.P. Tonner, Phys. Rev. B **49**, 15 370 (1994).
[61] P. Bruno, J. Phys. F **18**, 1291 (1988).
[62] D. Pescia, G. Zampieri, M. Stampanoni, G.L. Bona, R.F. Willis, and F. Meier, Phys. Rev. Lett. **58**, 933 (1987).
[63] C.M. Schneider, J. Kirschner, S.V. Halilov, and R. Feder (unpublished).
[64] T.M. Buck, G.H. Wheatley, and L. Marchut, Phys. Rev. Lett. **51**, 43 (1983).
[65] H. Niehus and C. Achete, Surf. Sci. **289**, 19 (1993).
[66] Since submission of the manuscript we performed preliminary STM investigations on our crystal in a different experimental system. On properly annealed surfaces we found average terrace widths between 500 and 1000 Å.
[67] S.T. Purcell, B. Heinrich, and A.S. Arrott, Phys. Rev. B **35**, 6458 (1987).
[68] J.J. de Miguel, A. Cebollada, J.M. Gallego, R. Miranda, C.M. Schneider, P. Schuster, and J. Kirschner, J. Magn. Magn. Mater. **93**, 1 (1991).
[69] A.K. Schmid and J. Kirschner, Ultramicroscopy **42-44**, 483 (1992).
[70] C.M. Schneider, A.K. Schmidt, P. Schuster, H.P. Oepen, and J. Kirschner, in *Magnetism and Structure in Systems of Reduced Dimension*, edited by R.F.C. Farrow, B. Dieny, M. Donath, A. Fert, and B.D. Hermsmeier (Plenum, New York, 1993), p. 453.
[71] K.E. Johnson, D.D. Chambliss, R.J. Wilson, and S. Chiang, Surf. Sci. **313**, L811 (1994).
[72] J. Giergiel (private communication).
[73] L.Z. Mezey and J. Giber, Jpn. J. Appl. Phys. **21**, 1569 (1982).
[74] Y.-L. He and G.-C. Wang, Phys. Rev. Lett. **71**, 3834 (1993).
[75] Q. Jiang, Y.-L. He, and G.-C. Wang, Surf. Sci. **295**, 197 (1993).
[76] A.M. Begley, S.K. Kim, J. Quinn, H. Over, and P.M. Marcus, Phys. Rev. B **48**, 1779 (1993).
[77] M.-T. Lin, J. Shen, J. Giergiel, W. Kuch, C.M. Schneider, and J. Kirschner (unpublished).
[78] J. Giergiel, J. Kirschner, J. Landgraf, J. Shen, and J. Woltersdorf, Surf. Sci. **310**, 1 (1994).
[79] C. Liu, E.R. Moog, and S.D. Bader, Phys. Rev. Lett. **60**, 2422 (1988).
[80] Y. Yafet and E.M. Gyorgy, Phys. Rev. B **38**, 9145 (1988).
[81] A. Kashuba and V.L. Pokrovsky, Phys. Rev. Lett. **70**, 3155 (1993).
[82] J.S. Earl, S.D. Brown, R.W. Chantrell, P.W. Haycock, and A. Lyberatos (unpublished).
[83] H.P. Oepen and J. Kirschner, Phys. Rev. Lett. **62**, 819 (1989).
[84] R. Allenspach, M. Stampanoni, and A. Bischof, Phys. Rev. Lett. **65**, 3344 (1990).
[85] H. Fritzsche, J. Kohlhepp, H.J. Elmers, and U. Gradmann, Phys. Rev. B **49**, 15 665 (1994).
[86] S. Chikazumi, *Physics of Magnetism* (Wiley, New York, 1964).
[87] B. Heinrich and J.F. Cochran, Adv. Phys. **42**, 523 (1993).
[88] C.M. Schneider, P. Bressler, P. Schuster, J. Kirschner, J.J.

de Miguel, R. Miranda, and S. Ferrer, Vacuum **41**, 503 (1990).
[89] H.P. Oepen, M. Benning, H. Ibach, C.M. Schneider, and J. Kirschner, J. Magn. Magn. Mater. **86**, L137 (1990).
[90] E.R. Moog, C. Liu, S.D. Bader, and J. Zak, Phys. Rev. B **39**, 6949 (1989).
[91] *Magnetic Properties of Metals*, edited by H.P.J. Wijn (Springer-Verlag, Berlin, 1991).
[92] W.A.A. Macedo, W. Keune, and E.D. Ellerbrock, J. Magn. Magn. Mater. **93**, 552 (1991).
[93] J.F. Cochran, J.M. Rudd, M. From, B. Heinrich, W. Bennett, W. Schwarzacher, and W.F. Egelhoff, Jr., Phys. Rev. B **45**, 4576 (1992).
[94] D.S. Chuang, C.A. Ballentine, and R.C. O'Handley, Phys. Rev. B **49**, 15 084 (1994).
[95] A. Berger, U. Linke, and H.P. Oepen, Phys. Rev. Lett. **68**, 839 (1992).
[96] J. Chen and J. Erskine, Phys. Rev. Lett. **68**, 1212 (1992).
[97] J. Giergiel, J. Shen, J. Woltersdorf, A. Kirilyuk, and J. Kirschner (unpublished).